SAR data and field surveys combination to update rainfall-induced shallow landslide inventory

Pietro Miele[a], Mariano Di Napoli[b*], Alessandro Novellino[c], Domenico Calcaterra[a], Jordi J. Mallorqui[d], Diego Di Martire[a,e]

[a] *Department of Earth, Environment and Resources Sciences, Federico II University of Naples, Complesso Universitario di Monte Sant'Angelo, Via Cinthia, 21 – 80126, Naples, Italy*

[b] *Department of Earth, Environmental and Life Sciences, University of Genoa, Corso Europa, 26 – 16132, Genoa, Italy*

[c] *British Geological Survey, Keyworth, NG12 5GG, Nottingham, UK*

[d] *CommSensLab-Universitat Politècnica de Catalunya, D3-Campus Nord-UPC, C. Jordi Girona 1-3, 08034, Barcelona, Spain*

[e] *Sintema Engineering srl – Spin-Off of the University of Naples Federico II, Via Toledo 156, 80134, Naples, Italy*

Corresponding author: mariano.dinapoli@edu.unige.it

Abstract

The *Campania* region has been recurrently hit by severe landslides in volcanoclastic deposits. The city of Naples, and in particular the *Camaldoli* and *Agnano* hills (Phlegraean Fields), also suffered several landslide crises in weathered volcanoclastic rocks as a consequence of intense rainfalls or wildfires. To identify slope failures phenomena occurred in the winter season 2019 – 2020 an innovative procedure has been proposed. The purpose of this procedure is to highlight areas where major land cover changes occurred within our area of study, which can be potentially related to mass movements. The amplitude of spaceborne SAR images has been exploited for the change detection analysis and the output derived from the segmentation procedure has been compared with field observations. The amplitude-based method has been already applied in the detection of landslides, but never on the event with limited extensions, such as for this application. The achieved outcomes allowed the mapping of 62 new landslides that have been used to update the current landslide inventory database. This type of information is expected to help decision-makers with land planning and risk assessment.

Keywords: amplitude imagery, synthetic aperture radar, landslides, rainfall, Naples

1. Introduction

The request for additional spaces in expanding cities and villages, driven by the continuous population increase, has led to deforestation and cut slopes (Altan et al. 2015; Gariano and Guzzetti 2016). These processes inevitably increase the incidence of landslides, by altering hydrological processes and shear-stress distribution (Wilkinson et al. 2002; Crosta and Frattini 2008). Landslide events globally result in tens of billions of US$ worth of damage and > 4300 lives lost annually (Froude and Petley, 2018). In Europe, and principally in Italy, slope failures represent the main cause of death produced by natural hazards (Guzzetti et al. 2012; Reichenbach et al. 2018). In Italy, only in 2019, 3 deaths and 27 injured have been reported and approximately 3,000 people evacuated or remained homeless while, from 1969 to 2020, about 1,100 deaths, 1,500 injured people and thousands of additional evacuees and homeless people have been recorded (https://polaris.irpi.cnr.it/report/last-report/).

Different studies have demonstrated the importance of available up-to-date and complete risk maps, which are based on Landslide Inventory Maps (LIMs), reducing the impact of these phenomena on society (Guzzetti et al. 2012). To this respect, it is noteworthy to mention that Italy is one of the very few countries in the world entirely covered with landslide susceptibility and risk maps since the beginning of the present century. However, considering the number of events (~620,000; ISPRA, 2018), there still is an urgent need to develop better tools for improving landslide risk management starting from the identification and mapping of landslides reported in the LIMs. The latter provides a detailed picture of landslides within an area by reporting location and, if known, date of occurrence and types of mass movements (Fell et al. 2008; Corominas et al. 2014). LIMs are basic elements in land-use planning and represent powerfully and easily understandable tools for researchers and authorities involved in landslide susceptibility analyses (Lombardo et al. 2015; Segoni et al. 2018; Di Napoli et al. 2020a, 2021; Arabameri et al. 2021; Yin et al. 2021) and landslide risk management (Dai et al. 2002; van Westen et al. 2006; Zhang et al. 2020). Regularly updating LIMs is a strategic activity for territorial planning, also considering that landslides can reactivate over time, even after long periods of quiescence (Guzzetti et al. 2012; Solari et al. 2020).

Over the last three decades, Remote Sensing (RS) technologies based on satellite optical and Synthetic Aperture Radar (SAR, Franceschetti et al. 1992) imagery have been used for landslides detection and mapping (Stumpf et al. 2017; Novellino et al. 2017; Del Soldato et al. 2018; Guerriero et al. 2019). Differently from optical images, SAR sensors have the advantage to be able to gather ground surface information regardless of weather and illumination conditions. Geoscientists have widely exploited Interferometric SAR (InSAR, Gabriel et al. 1989) techniques to resolve the spatial distribution and temporal evolution of ground instabilities by considering phase values associated with SAR scenes (Novellino et al. 2015; Confuorto et al. 2017; Raspini et al. 2017; Spinetti et al. 2019). Due, to the inherent limitations of current space observation systems and data processing techniques (Colesanti and Wasowski 2006; Wasowski and Bovenga 2014), InSAR approaches are mostly applicable to extremely slow ($<$16mm/yr) and very-slow movements (≥1.6mm/yr and ≤16mm/yr) landslides (Cruden and Varnes 1996) which typically correspond to deep-seated gravitational slope deformations, creep, and, in some cases, slides and complex landslides (Saroli et al. 2005; Di Martire et al. 2016; Bozzano et al. 2017). Recent studies have used interferograms to detect precursor signals of fast movement landslides (falls and topples) or to identify areas where a mass movement has potentially occurred (Barra et al., 2016; Casagli, 2017; Kyriou & Nikolakopoulos, 2018).

To map deformations induced by relatively rapid landslides, the analysis of amplitude signal associated with the SAR images can be an effective alternative (Mondini et al. 2019). Amplitude-based methods analyse the changes across two images (pre-and post-event) induced by a landslide. Despite changes in SAR amplitude have been already used to monitor land cover (Freitas et al. 2008; Qi et al. 2012), many studies have demonstrated the valuable contribution of this approach to detect landslides (Mondini et al. 2017). Still, fewer are applications of polarimetric SAR based on amplitude information data for landslides mapping which are limited to large landslides, typically in the order of km^2 of extension (Shimada et al. 2014; Plank et al. 2016). In this work, amplitude-based methods were explored to map landslides with limited extension (hundreds of square meters).

Such a semi-automatic procedure aims at highlighting land cover changes (potentially related to rapid-moving landslides) by exploring radar backscattered signals differences in consecutive spaceborne SAR images. The mass movement phenomena occurred during the 2019 – 2020 winter season in the *Agnano* plain and *Camaldoli* hill located within the city of Naples (*Campania* region, southern Italy, Figure 1) were analysed. Most of these events-were triggered by high-intensity and short-duration precipitations or prolonged rainfalls affecting the most superficial loose pyroclastic deposits.

The paper is organized as follows: first, the geological and geomorphological setting of Naples' municipality area is presented. The data and methods used in the work are successively analysed. Further, an overview of basic concepts of the polarimetric SAR amplitude technique is described. Finally, polarimetric outcomes are compared with field surveys data to evaluate the applicability of the semi-automatic procedure to landslide detection.

2. Study area

The *Agnano* plain and *Camaldoli* hill are located in the eastern sector of the Phlegraean Fields, a ~450 km^2 active volcanic area located in the western sector of the city of Naples. The area has experienced numerous eruptions from monogenic volcanoes over the past 70,000 years (Scarpati et al. 2013, 2015,

Figure 1) with the local landscape and bedrock geology mainly shaped by two eruptions: Campanian Ignimbrite eruption (CI - occurred 39,000 years; Rolandi et al., 2020) and the Neapolitan Yellow Tuff eruption (NYT- occurred 15,000 years ago; Scarpati et al., 2013). These sequences are covered by pyroclastic, anthropogenic, and epiclastic deposits with abrupt variations in thickness and facies that have proven to be very susceptible to landslides (Calcaterra et al., 2007).

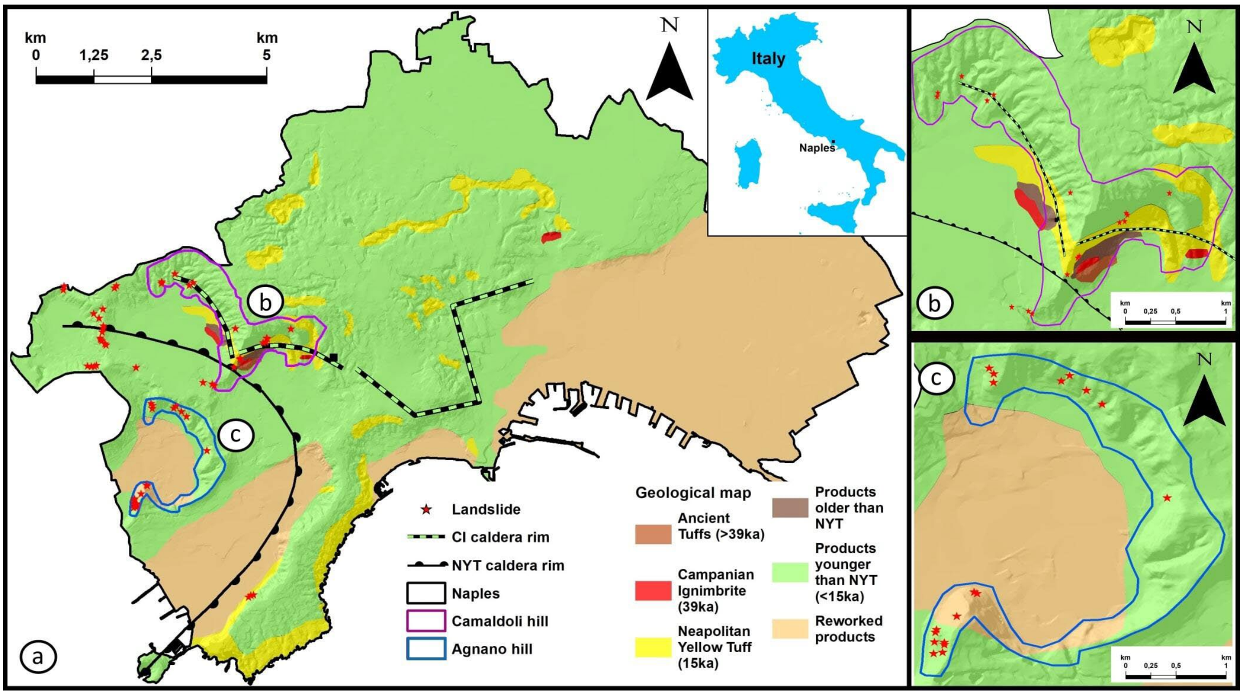

Figure 1. a) Geological sketch map of the urban area of Naples (modified from Scarpati et al. 2015); b) and c) detailed view of *Camaldoli* hill and *Agnano* plain, respectively (western sector of city of Naples, purple and blue bold lines in a).

The morphology of the whole Phlegraean area reflects the evidence of volcano-tectonic Quaternary events and the slopes are the remains of ancient volcanic buildings. These hills consist of several tens of metre thick NYT and are generally covered by younger (< 15 ka) loose and unconsolidated pyroclastic deposits (Ascione et al. 2020). Additionally, the energy of relief is quite high where local hills are characterized by high slope angles (> 30°). The caldera inner slopes have typical semi-circular planar shapes and steep profiles that make them prone to landsliding (Calcaterra et al. 2007; Ascione et al. 2020). Also, the drainage network presents a pronounced structural control, where low-order straight channels are exposed (Di Martire et al. 2012). Sea level variations also greatly contributed to the present morphological setting. These conditions have represented predisposing factors for the development of landslides since the Roman era (Morra et al. 2010).

Landslides are the main geomorphic processes within Naples municipality. Although landslides have generated disruption and damage over time, only in recent decades more attention has been posed to these phenomena, following the February 1986 rainfall event, representing a threshold between historical and recent mass movements (Beneduce et al. 1988; Calcaterra et al. 2002; Di Martire et al. 2012) which led to complete landslide inventory in the Phlegraean area (Carratù et al. 2015; Finicelli et al. 2016). The inventories reveal that landslides mostly affect the shallow pyroclastic cover and have thicknesses in the order of 0.5 to 2 m (Calcaterra et al. 2007) and are characterized by relatively low mobility.

3. Materials and methods

The procedure for the individuation and validation of the landslides consists in two independent steps. The former includes the identification of slope failures through field surveys and Google Earth images inspection leading to a creation of a landslide inventory, while the latter is characterized by the collection and processing of radar polarimetric satellite images for the development of another landslide inventory. Finally, the two outputs have been compared to assess the results (Figure 2).

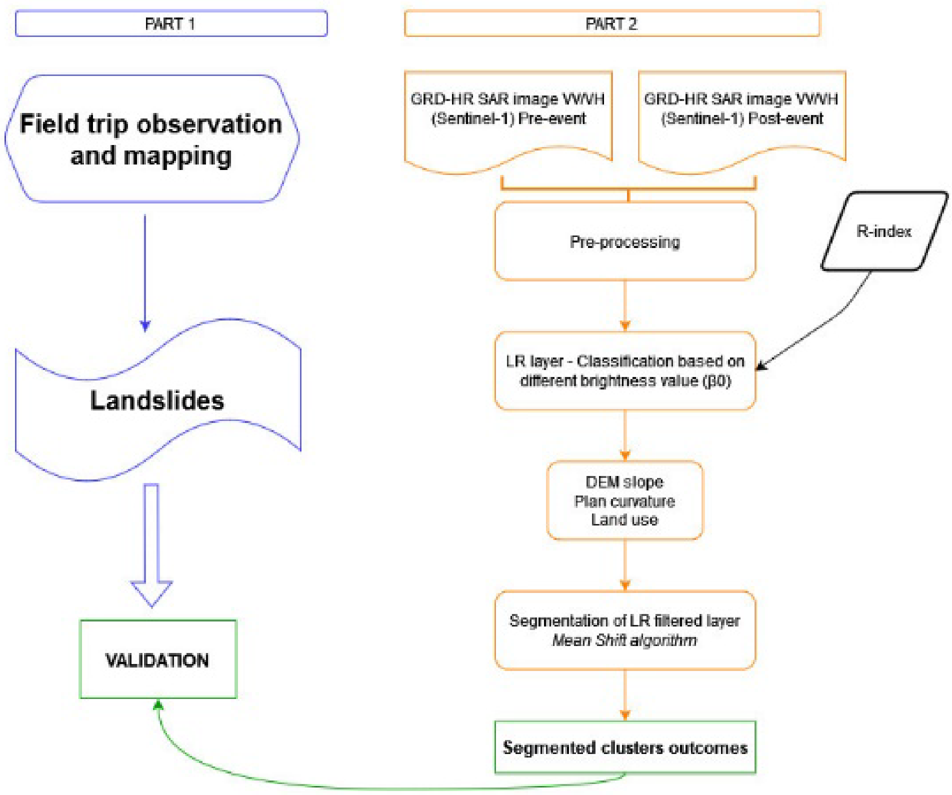

Figure 2. Flowchart of the proposed methodology. Additional information on part 2 are provided in Section 3.2.

3.1 On-site investigation data

Landslide inventories represent essential input data to implement any study on landslide susceptibility, hazard or risk assessment. Very often this data is missing or not homogeneous in space and time, leading to an incorrect evaluation of the above-mentioned analyses. In the investigated area, several studies have already compiled a partial census of landslide phenomena (Calcaterra et al. 2002; Di Martire et al. 2012; Carratù et al. 2015; Finicelli et al. 2016) in addition to the *I.F.F.I.* (Landslide Inventory in Italy) national landslides database.

This database covers a time span of about two centuries (1816 - 2015) and is based upon field surveys, aerial photo interpretation and local and national archival research of relevant sources (Di Martire et al., 2012). As a result, about 1300 landslides were inventoried and classified as “historical” or “recent” conventionally using the February 1986 event as a temporal divide. The main flaw of this database is the lack of consistency in space and time, the different methodologies adopted and the different classification criteria used.

Winter season 2019 – 2020 has been characterized by the occurrence of several high-intensity and short-duration rainfalls, where one of the most severe recorded values of 66 mm of cumulative rainfall in 30 minutes. Such events have triggered many slope failures and undermining surface drainage systems in urban areas. As a consequence, visual interpretation of Google Earth images integrated by geomorphological field survey observations were performed to validate and update the landslide inventory with the latest mass movements that occurred in the area. Field surveys were carried out on topographical maps at 1:5,000 scale from December 2019, following the intense rainfall phenomena that occurred in the Phlegraean area. Based on the adopted scale, only landslides larger than 25 m^2 were considered.

3.2 Visibility maps

SAR images are very useful tools for detecting and monitoring land cover changes but, being sensed in a side-looking configuration (Kropatsch and Strobl 1990), it is important to predict if the measurements over the study area might be affected by geometrical distortions before any processing. A preliminary analysis was carried out to obtain the Range Index (RI) (Notti et al. 2012, 2014), the latter is a pixel-by-pixel representation of the relationship between the geometry of acquisition of the satellite (slant range) and the topography Slope angle (S) and slope Aspect (A); (Plank et al. 2012; Del Soldato et al. 2021). The RI was applied to the Level-1 GRD products before part 1 in order to assess the quality of the pixels in the area of interest and to select the most effective stack to process. The elements needed to calculate the RI are a DEM and the satellite Line of Sight (LoS) parameters, namely the incidence angle (α) and heading (θ). The maximum value of RI is 1. This occurs when the slope is parallel to the LoS. This is the best geometry to obtain SAR features in mountainous areas. On the contrary, the lowest value of RI occurs in the case of foreshortening ($0 < RI < 0.3$) or layovering (RI < 0) effects. Obtained outcomes have been classified according to the four main RI classes suggested by Notti et al. (2012).

3.3 SAR images processing

The pre-processing procedure is based on Sentinel-1 images acquired in the Level-1 Ground Range Detected – High Resolution format (GRD-HR) and Interferometric Wide acquisition mode in VV and VH polarization (https://scihub.copernicus.eu/). Level-1 GRD products are focused SAR data that has been multi-looked and projected to ground range using the Earth ellipsoid model WGS84. Only the amplitude information associated with each pixel in the image was considered (https://sentinel.esa.int/web/sentinel/missions/sentinel-1/data-products). The resulting product has squared pixels of 10 m resolution with reduced speckle.

For the purpose of this work, six images were acquired shortly after the heaviest rainfall recorded in the area, both in ascending and descending orbit and covering the period between 17 September 2019 and 16 January 2020 (Table 1).

Table 1. Analysed SAR imagery in the amplitude change detection. The listed products correspond only to images acquired in descending orbit. The whole considered imagery dataset corresponds to GRD-HR dual-pol products.

Date	Satellite platform
17 September 2019	Sentinel-1B
5 October 2019	Sentinel-1A
5 November 2019	Sentinel-1B
4 December 2019	Sentinel-1A
29 December 2019	Sentinel-1A
16 January 2020	Sentinel-1A

Pre-processing of the images is performed to obtain Beta Nought (β_0), namely the radar brightness coefficient in slant coordinates. This part is done using the open-source software SNAP, available through the European Space Agency (https://step.esa.int/main/download/snap-download/), and includes the following steps: retrieving the precise orbits, removing the thermal noise and radiometric calibration (Filipponi 2019). SAR images were co-registered with a 10 m Digital Elevation Model (DEM)-assisted procedure (Tarquini et al. 2007). After the co-registration, the resulting stacked images are filtered for speckling reduction using the adaptive Frost filter (Frost et al. 1982), with a filter size in X and Y of 5 pixels, and a damping factor of 2.

3.4 SAR amplitude changes detection

SAR backscatter is dependent on a number of factors, including the polarization and wavelength used by the SAR system, the local slope orientation relative to the SAR sensor and the roughness and dielectric properties (e.g. soil moisture, presence of vegetation) of the material that the microwave energy interacts with at the Earth's surface (Burrows et al., 2022).

Analysing changes between pre-and post-event amplitude SAR images is based on the assumption that landslides change the local land cover and its backscattering properties. For instance, when a mass movement occurs, if the mobilised material covering the previous surface is characterized by a higher moisture content then the backscatter signal should increase (Novellino et al. 2020). Back-scattering might also increase when the surface roughness (at the scale of the used wavelength) increases (Oliver and Quegan 2004) for example as a result of trees being ripped off leaving bare soil or rock. Following the procedure defined by Mondini (2017), the Log-Ratio (LR) index was then computed in every pixel for each couple of dual-pol consecutive images. LR index estimates change in brightness that can be induced by land cover changes due to both natural (e.g., landslides, floods, snow melting) or human-induced activities (e.g., deforestation, mining activities) in a defined time interval. The obtained ratio image helps suppressing background structures and improve the detectability of potential changes from SAR data (Ajadi et al., 2016).

For each pair of corresponding pixels belonging to consecutive pre-processed SAR images, LR is calculated as follows (Esposito et al. 2020, Eq. 1):

$$LR = \ln\left(\frac{\beta_{0,i}}{\beta_{0,i-1}}\right) \qquad \text{(Eq. 1)}$$

where β_0 is the reflectivity per unit area in slant range; its values are independent from the terrain covered and *i-th* image indicate two consecutive pre-processed SAR images. LR pixels can assume by positive or negative values, depending on the backscattering changes. Then, a subset of Region of Interest (RoI) is extracted by using the subset tool in SNAP.

3.5 Image segmentation and matching assessment

Before the segmentation, a filtering step has been performed to mask pixels that cannot correspond to landslides (i.e., flat urban areas). In fact, to obtain an LR filtered layer, areas potentially affected by mass movements were separated using morphological parameters derived from slope and plan curvature. Additionally, areas in shadowing and foreshortening in the RI have been masked out and removed. Moreover, to ensure the correct identification of urban boundaries, land-use information derived from the second level of the 2018 Corine Land Cover (CLC) program were taken into account (https://land.copernicus.eu/pan-european/corine-land-cover/clc2018). CLC classification system is hierarchical and subdivided into different levels: the second level of the CLC classification for the urban group includes areas mainly occupied by dwellings and buildings used by administrative/public utilities, including their connected areas (associated lands, approach road network, parking lots).

LR layer segmentation groups pixels with similar LR values into various unique segments. The image is partitioned into regions that contain points having nearly the same properties, e.g. mean values or textural properties (Tang 2010). In this work, the segmentation process is performed with the "*i.segment*" module in GRASS GIS 7.8.3 using the "Mean Shift" algorithm and the adaptive bandwidth option (Fukunaga and Hostetler 1975).

For the segmentation of the filtered LR, the algorithm requires the definition of the following parameters: *i*) a selective threshold with a value between 0 and 1; *ii*) the kernel size; *iii*) the minimum number of cells falling into a cluster and *iv*) the minimum number of iterations. A threshold of 0 would allow only pixels with identical values to be considered similar and clustered together in a segment, while a threshold of 1 would allow everything to be included in a large segment (Momsen and Metz 2017). Mean Shift algorithm recalculates central pixel values using the user-defined maximum number of iterations or until the shift between the central pixel and pixels within the kernel results is smaller than the user-defined threshold. The threshold choice depends on the purpose of the application and the image resolution (Comaniciu and Meer 1999; Tao et al. 2007). To select the appropriate parameter values, iterative steps have been carried out manually. According to Esposito et al. (2020), the criterion for selecting the best input values is to search for the combination of values that optimize, at the same time, the number of clusters and their average size concerning the expected land cover changes. To avoid over-segmentation, a threshold value of 0.1 has been chosen and a minimum of 3 pixels has been used as criteria to determine the presence of a cluster with the Euclidean calculation method. Considering the approximate expected size of the land cover changes, the size of the spatial kernel was set to 10 pixels with 200 iterations to detect significant differences in LR values and to minimize the "*salt and pepper effect*" both for VH and VV polarization LR layers.

The obtained outcomes have been matched with the surveyed data reported in the LIM map. This procedure allowed to compare the two datasets in terms of the number of landslides recognized and their areal extension.

4. Results and discussion

4.1 On-site investigation outcomes

The field inspection was conducted into the whole municipality of Naples by using Google Earth images as ancillary data (Figure 3). Through this examination, 62 landslides were recognized and added to the previous landslide inventories available for the city of Naples (Di Martire et al, 2012; Carratù et al., 2015; Finicelli et al., 2016), bringing the total number of phenomena surveyed to 1322. Of the 62 new mass movements, 29 are located on the slopes of the *Agnano* plain and the *Camaldoli* hill so confirming that these areas have the highest susceptibility within Naples (Figure 1b). According to Cruden and Varnes (1996) classification, the detected slope failures can be classified as rotational or translational slides, which are typical phenomena affecting local hilly areas, particularly in case of prolonged or intense rainfall events. In fact, considering the geological and geomorphological setting of the Phlegraean Field, rainfall is the main triggering factor of mass movements (Calcaterra et al., 2000; Fusco et al., 2019) and between September and December 2019, the *Campania* region was affected by several rainfall events of high intensity and short duration (http://centrofunzionale.regione.campania.it). Moreover, by consulting the reports on hydrological events, it was possible to note that, especially in September 2019, the city of Naples was hit by severe precipitation. From field observations, it was noted that the tuffs are affected by falls and topples, which move from high-angle walls and, more frequently, from cut slopes or quarry walls (Calcaterra et al. 2002). Moreover, many landslides with complex evolution can be observed along the Phlegrean hilly slopes. These phenomena are characterized by localized residual movements and occasional reactivations.

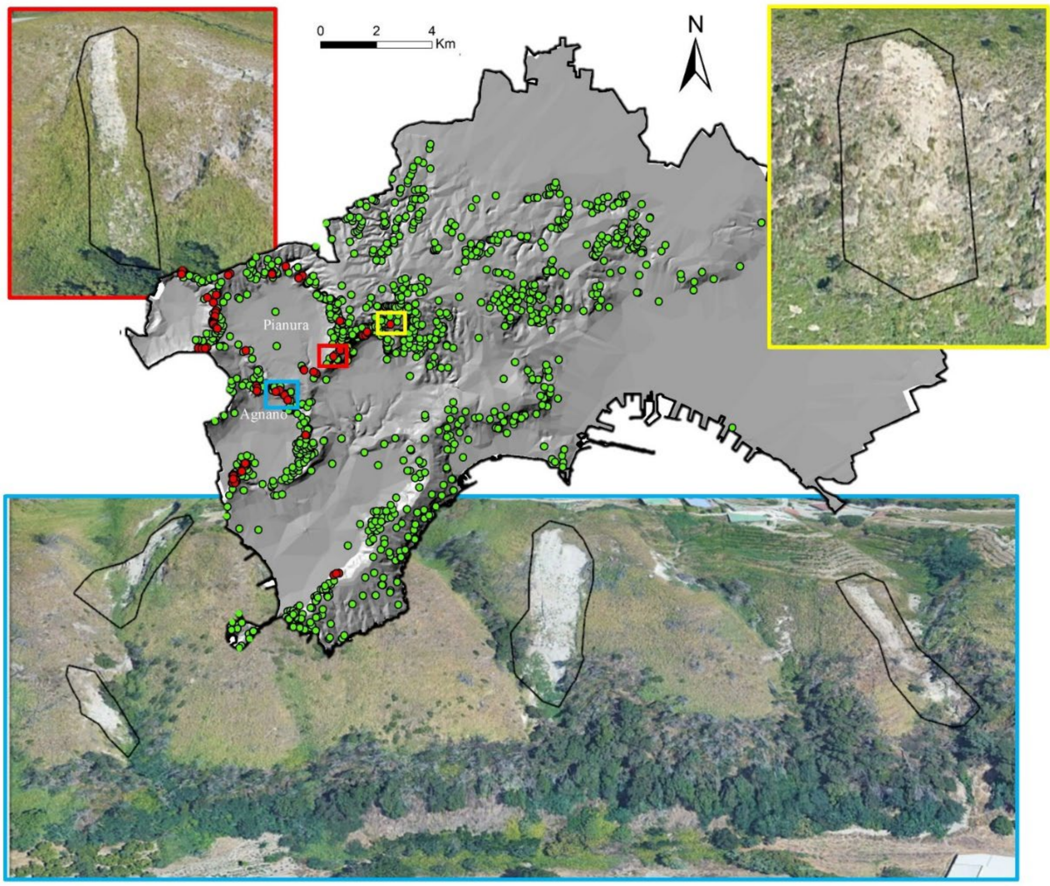

Figure 3. Landslide inventory map for the Naples municipality where red dots show the new surveyed landslides, whereas, green ones indicate the mass movements already obtained from official inventories. The black polygons refer to the outcome obtained with the segmentation step.

Hence, different change detections have been accomplished to identify the number of landslides associated with the different rainfall events and to create a multi-temporal catalogue of the mass movements triggered in the study area.

The heavy rainfalls and severe wildfires, together with land-use changes (i.e., abandonment of agricultural practices; Figure 4) have caused a progressive increase in landslide occurrence over time. These problems combined with the urban sprawl has increased the landslide risk in this context (Calcaterra et al. 2007).

Figure 4. Interaction between land-use change (green) and landslides (light red). Lateral landslides were detached at the base of the terraced areas where the agricultural practices are still active, differently from the central landslide.

4.2 Change detection analyses

The preliminary analysis based on the RI calculation shows that most of the slopes in the *Agnano* and *Camaldoli* areas is affected by topographic effects limiting SAR applications (Figure 5). The ascending orbit is characterized by a low RI (< 0.3) affected by foreshortening and the terrain geometry has a high impact on the backscattered signal, then limiting the effectiveness of the amplitude analysis on the ascending stack that has been, therefore, excluded. As shown in Figure 5, the western side of *Camaldoli* hill and almost all of the *Agnano* slopes fall into a low RI class. By comparing ascending and descending orbits, it is possible to note that the descending geometry is better suited for slopes facing West. On the contrary, the ascending geometry allows to better investigate slopes oriented to the East. Considering the western wards landslides' directions of motion, only descending SAR images have been employed in this work.

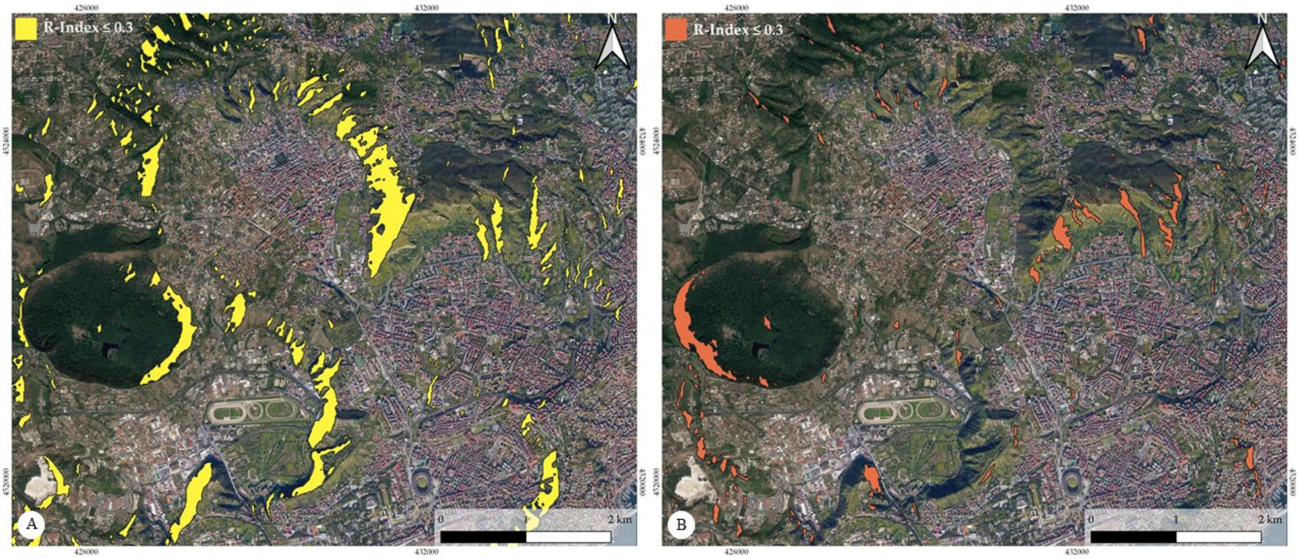

Figure 5. R-Index maps of *Camaldoli* hill and *Agnano* plain in the ascending geometry (a) and descending geometry (b). In ascending geometry most of the slopes are affected by layover and shadowing problems due to the topography effects and LoS parameters.

Subsequently, LR has been filtered by selecting out flat urban areas. In our study area, flat areas correspond to built-up zones while the unstable slopes involve only vegetated areas. For this reason, urban areas have not been considered, while acknowledging that mass movement phenomena can also be triggered in urban contexts (Di Napoli 2020b, Novellino et al., 2021, Miele et al., 2021).

After the segmentation of the LR filtered layer, segments with a minimum size of 3 pixels, corresponding to a minimum area of 300 m^2, were extracted in the RoI. The output of the segmentation algorithm returned 39 clusters in the *Camaldoli* and *Agnano* areas (Figure 6). The obtained outcomes correspond to small and isolated clusters (black pixels) in a homogeneous region, where the backscattering variations were most significant ($\Delta\beta_0$ ranging from 0.6 and 0.7). In large parts of the investigated area, there weren't significant variations in terms of the backscattered signal and these outputs have been interpreted taking into account the geometry of the cluster. Namely, clusters running perpendicular to the line of the maximum slope were not considered as well as clusters that cover areas too large are not compatible with the typical landslides historically occurred in the study area.

Concerning the multi-temporal analysis, different change detections were analysed considering different images acquired at monthly intervals. Specifically, in the period between September and October two landslides were recorded on the *Camaldoli* hill while four phenomena were identified between October and November in *Agnano*. Between November and December, a total of five landslides were identified in *Agnano* (i.e., 3) and *Camaldoli* (i.e., 2) and finally, the eleven events were mapped between December 2019 and January 2020 on the slopes of the *Agnano* plain (Table 2 and Figure 6).

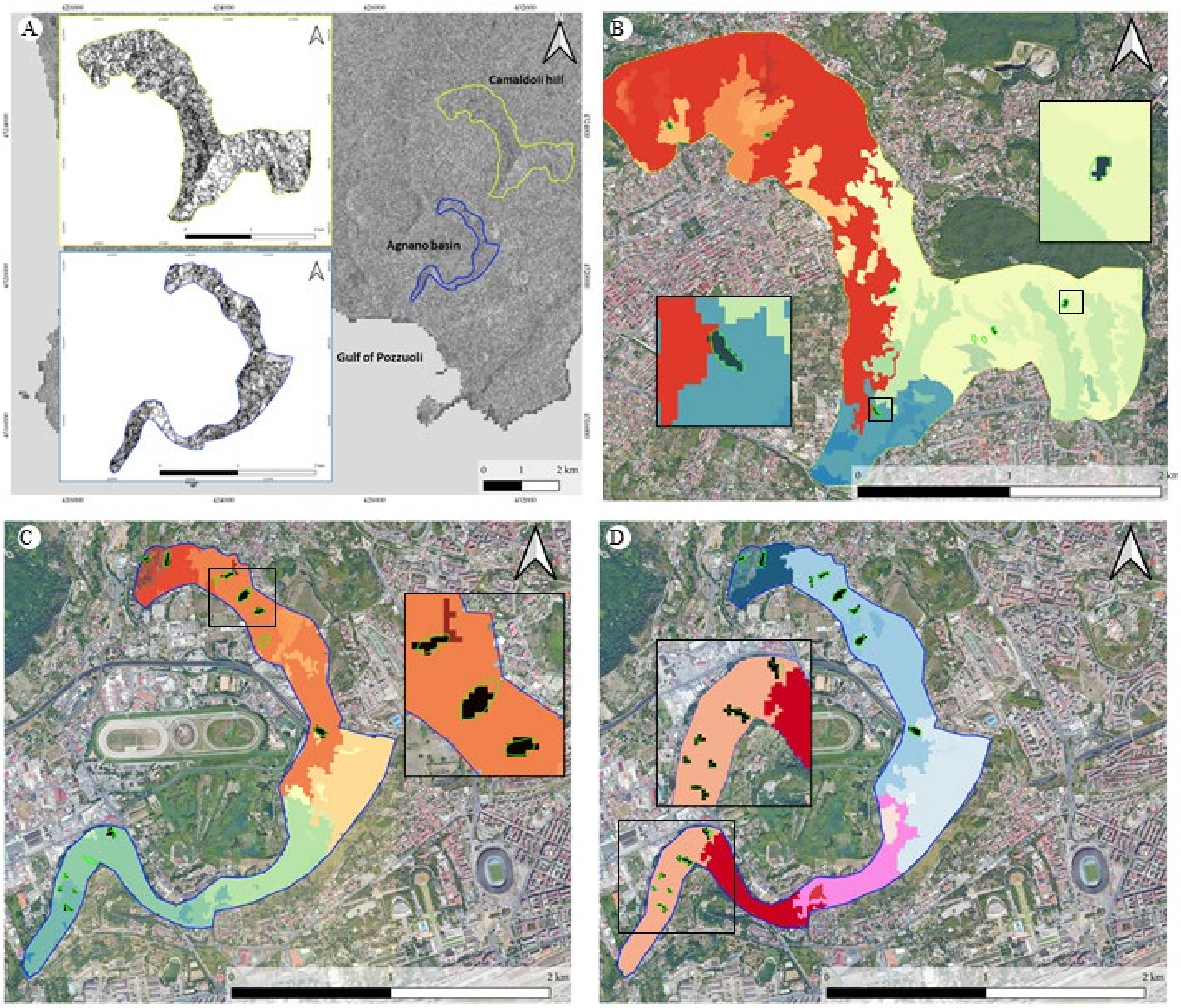

Figure 6. Outputs from the segmentation step: a) LR amplitude layer of the RoI within part of Phlegrean Fields obtained stacking the last two SAR images considered (29 December 2019 and 16 January 2020) clipped around the *Agnano* plain and *Camaldoli* hill areas; b) segmentation results for the October-November period in the *Camaldoli* hill; c) results for the December-January period over the *Agnano* plain; d) results for December at the *Agnano* plain. The background different colours represent the segmentation output and green polygons correspond with the mass movements shape surveyed. Potential pixels associated with landslides, detected after the segmentation, are represented with the same colour (i.e., black).

Table 2. Summary of landslides recognition for each change analysis computed.

TIME SPAN	*AGNANO*	*CAMALDOLI*
SEPTEMBER/OCTOBER	-	2
OCTOBER/NOVEMBER	4	-
NOVEMBER/DECEMBER	3	2
DECEMBER/DECEMBER	-	5
DECEMBER/JANUARY	11	-
SUM OF CHANGE DETECTION	18	9

4.3 SAR and field surveys comparison

Twenty-seven out of the 39 clusters individuated with the segmentation process correspond to landslides detected in the field. The remaining 12 clusters could be interpreted as False-Positive (FP), because small landslides can be immediately obliterated or the amplitude-based method might detect slope failures in areas inaccessible to survey, or False-Negative (FN) due to limited spatial resolution of the SAR products. FP and FN have been also considered in the comparison analysis. Both FP and FN, as well as validated landslides, are located near the slope breaks and in correspondence of relatively high acclivity (i.e., greater than 35°). In particular, on the *Camaldoli* slopes have been identified 2 FN and 5 FP, whereas, in *Agnano* plain have been recognized 2 FN a 3 FP. True Positives (TP) correspond to 78.8% and, if landslides >300 m^2 are taken into account, TP increases to 80% (Figure 7).

The recognised clusters show an areal extent of landslide slopes larger than the areas mapped during the field survey. This overestimation is unfortunately due to the low satellite images resolution that, when small landslides occur, do not allow the exact delimitation of the landslide area (East sector of *Camaldoli* hill, Figure 7).

As already discussed in a previous similar study (Barra et al., 2016), the use of interferometric processing for landslide detection was proved. The main add-on of the current study regards the amplitude-based approach to prove the likelihood to map the scars caused by the landslide. However, this approach could be particularly useful in rapid landslide investigation allowing precise identification of landslides location, especially when are present area inaccessible to field detectors, as demonstrated on *Camaldoli* hill.

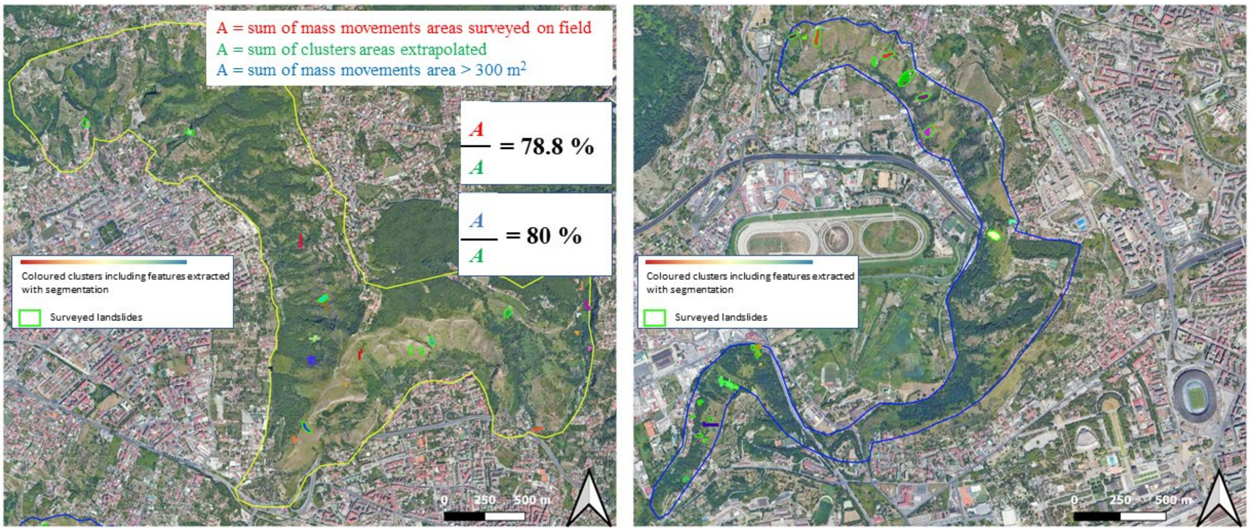

Figure 7. Comparison between the SAR derived segmentation map and the field investigation. In the *Agnano* plain (right) there is a good correspondence between landslides' shapes and clusters. The *Camaldoli* hill area presents many clusters corresponding to false-positive objects due to issues of visibility parameters (see visibility maps).

5. Conclusions

Over the last decades, remote sensing technologies have supported landslide monitoring and detection analyses at relatively low costs. Among them, amplitude-based methods have been employed in very large mass movements identification. A semi-automatic procedure to identify rapid landslide occurrence in measures of SAR amplitude changes has been tested in this work in the outskirts of

Naples (Italy). The scope of our method is to obtain preliminary information from radar imagery on mass movements when atmospheric conditions (cloud coverage) prevent the use of optical images. However, in the presented analyses all the data and software adopted are completely free-of-charge. For the chosen study area, only SAR images acquired in descending orbit were considered due to the geometrical constraints recorded in the ascending orbit. At the same time, extensive field surveys activities have been executed in the study area. The results obtained, with 27 events confirmed by field surveys, assert that SAR Sentinel-1 images are successful in capturing rapid landslides. SAR images permit to obtain quick and reliable information in supporting disaster management civil protection operations on landslides occurrence following a rain event. Moreover, in bibliography, polarimetric applications have been already presented focusing on very huge mass movements detection. As shown in the results section, it is possible to identify also landslides with limited extension (hundreds of square meters) which are more likely in the Phlegrean setting. Further applications could be implemented by using SAR images with a very high resolution allowing more accurate results.

The integration between RS and conventional geological methods can represent a significant tool for intervention works planning, providing the right indication on how and where to operate to reduce the risk and to increase the safety of the area.

Author Contributions: Conceptualization, P.M., M.D.N., A.N., D.D.M.; data curation, P.M., M.D.N., A.N.; formal analysis, P.M., M.D.N., A.N.; investigation, M.D.N, D.D.M., D.C.; methodology, P.M., M.D.N., A.N., D.D.M.; software P.M., A.N.; validation, M.D.N., D.D.M., D.C.; writing – original draft preparation P.M., M.D.N., A.N.; writing – review and editing, D.D.M., J.M., D.C.; supervision, D.D.M. all authors have read and agreed to the published version of the manuscript.

Funding: The work was funded by the scholarship "P.O.N. Dottorati innovativi a caratterizzazione industriale 2014-2020" and by the Spanish MICIN, the State Research Agency (AEI) under projects TEC2017-85244-C2-2-P and PID2020-117303GB-C21 MCIN/AEI/10.13039/501100011033.

Data Availability Statement: For consulting the reported results, it's possible to contact Mariano Di Napoli.

Acknowledgments: The authors thank Consorzio interUniversitario per la prevenzione dei Grandi Rischi (CUGRI) for providing technological support. In addition, the authors would like to thank the anonymous reviewers for their valuable and insightful comments to improve the paper.

Conflicts of Interest: The authors declare no conflicts of interest.

References

Altan O, Alcántara-Ayala I, Baker D, et al (2015) Disaster Risks Research and Assessment to Promote Risk Reduction and Management. Sociology & Anthropology Department Faculty Publications

Arabameri A, Pal SC, Rezaie F, et al (2021) Decision tree based ensemble machine learning approaches for landslide susceptibility mapping. Geocarto International 0:1–35. https://doi.org/10.1080/10106049.2021.1892210

Ascione A, Aucelli PPC, Cinque A, et al (2020) Geomorphology of Naples and the Campi Flegrei: human and natural landscapes in a restless land. Journal of Maps 0:1–11. https://doi.org/10.1080/17445647.2020.1768448

Barra, A., Monserrat, O., Mazzanti, P., Esposito, C., Crosetto, M., & Scarascia Mugnozza, G. (2016). First insights on the potential of Sentinel-1 for landslides detection. Geomatics, Natural Hazards and Risk, 7(6), 1874-1883

Beneduce P, D'elia G, Guida M (1988) Morfodinamica dei versanti dell'area Flegrea (Campania) : Erosione in massa ed erosione lineare. Memorie della Societa Geologica Italiana 41:949–961

Bozzano F, Mazzanti P, Perissin D, et al (2017) Basin Scale Assessment of Landslides Geomorphological Setting by Advanced InSAR Analysis. Remote Sensing 9:267. https://doi.org/10.3390/rs9030267

Burrows, K., Marc, O. and Remy, D., 2022. Establishing the timings of individual rainfall-triggered landslides using Sentinel-1 satellite radar data. Natural Hazards and Earth System Sciences Discussions, pp.1-24. https://doi.org/10.5194/nhess-2022-21 [in review]

Calcaterra D, Coppin D, de Vita S, et al (2007) Slope processes in weathered volcaniclastic deposits within the city of Naples: The Camaldoli Hill case. Geomorphology 87:132–157. https://doi.org/10.1016/j.geomorph.2006.03.040

Calcaterra D, de Riso R, Nave A, Sgambati D (2002) The role of historical information in landslide hazard assessment of urban areas: the case of Naples (Italy). In: Proc. 1st European Conf. on Landslides, Prague, Czech Republic, 24–26 June 2002

Calcaterra, D., Parise, M., Palma, B., & Pelella, L. (2000). The influence of meteoric events in triggering shallow landslides in pyroclastic deposits of Campania, Italy. In Landslides in Research, Theory and Practice: Proceedings of the 8th International Symposium on Landslides held in Cardiff on 26–30 June 2000 (pp. 1-209). Thomas Telford Publishing

Carratù MT, Di Martire D, Finicelli GF, Calcaterra D (2015) Comparison of bivariate and multivariate analyses for landslide susceptibility mapping in the Phlegraean district: the case study of Camaldoli hill (Napoli, Italy). Rend Online Soc Geol It 35:50–53. https://doi.org/doi: 10.3301/ROL.2015.61

Casagli, N., Tofani, V., Morelli, S., Frodella, W., Ciampalini, A., Raspini, F., & Intrieri, E. (2017). Remote sensing techniques in landslide mapping and monitoring, keynote lecture. In workshop on world landslide forum.

Colesanti C, Wasowski J (2006) Investigating landslides with space-borne Synthetic Aperture Radar (SAR) interferometry. Engineering Geology 88:173–199. https://doi.org/10.1016/j.enggeo.2006.09.013

Comaniciu D, Meer P (1999) Mean shift analysis and applications. In: Proceedings of the Seventh IEEE International Conference on Computer Vision. pp 1197–1203 vol.2

Confuorto P, Di Martire D, Centolanza G, et al (2017) Post-failure evolution analysis of a rainfall-triggered landslide by multi-temporal interferometry SAR approaches integrated with geotechnical analysis. Remote Sensing of Environment 188:51–72. https://doi.org/10.1016/j.rse.2016.11.002

Corominas J, van Westen C, Frattini P, et al (2014) Recommendations for the quantitative analysis of landslide risk. Bull Eng Geol Environ 73:209–263. https://doi.org/10.1007/s10064-013-0538-8

Crosta GB, Frattini P (2008) Rainfall-induced landslides and debris flows. Hydrological Processes 22:473–477. https://doi.org/10.1002/hyp.6885

Cruden DM, Varnes DJ (1996) Landslides: Investigation and Mitigation. Chapter 3 - Landslide types and processes. Transportation Research Board Special Report

Dai FC, Lee CF, Ngai YY (2002) Landslide risk assessment and management: an overview. Engineering Geology 64:65–87. https://doi.org/10.1016/S0013-7952(01)00093-X

De Luca C, Furcolo P, Rossi F, et al (2010) Extreme rainfall in the mediterranean. 9

Del Soldato M, Riquelme A, Bianchini S, et al (2018) Multisource data integration to investigate one century of evolution for the Agnone landslide (Molise, southern Italy). Landslides 15:2113–2128. https://doi.org/10.1007/s10346-018-1015-z

Del Soldato M, Solari L, Novellino A, et al (2021) A New Set of Tools for the Generation of InSAR Visibility Maps over Wide Areas. Geosciences 11:229. https://doi.org/10.3390/geosciences11060229

Di Martire D, De Rosa M, Pesce V, et al (2012) Landslide hazard and land management in high-density urban areas of Campania region, Italy. Nat Hazards Earth Syst Sci 12:905–926. https://doi.org/10.5194/nhess-12-905-2012

Di Martire D, Novellino A, Ramondini M, Calcaterra D (2016) A-Differential Synthetic Aperture Radar Interferometry analysis of a Deep Seated Gravitational Slope Deformation occurring at Bisaccia (Italy). Science of The Total Environment 550:556–573. https://doi.org/10.1016/j.scitotenv.2016.01.102

Di Napoli M, Carotenuto F, Cevasco A, et al (2020a) Machine learning ensemble modelling as a tool to improve landslide susceptibility mapping reliability. Landslides. https://doi.org/10.1007/s10346-020-01392-9

Di Napoli M, Di Martire D, Bausilio G, et al (2021) Rainfall-Induced Shallow Landslide Detachment, Transit and Runout Susceptibility Mapping by Integrating Machine Learning Techniques and GIS-Based Approaches. Water 13:488. https://doi.org/10.3390/w13040488

Di Napoli M, Marsiglia P, Di Martire D, et al (2020b) Landslide Susceptibility Assessment of Wildfire Burnt Areas through Earth-Observation Techniques and a Machine Learning-Based Approach. Remote Sensing 12:2505. https://doi.org/10.3390/rs12152505

Esposito G, Marchesini I, Mondini AC, et al (2020) A spaceborne SAR-based procedure to support the detection of landslides. Natural Hazards and Earth System Sciences 20:2379–2395. https://doi.org/10.5194/nhess-20-2379-2020

Fell R, Corominas J, Bonnard C, et al (2008) Guidelines for landslide susceptibility, hazard and risk zoning for land-use planning. Engineering Geology 102:99–111. https://doi.org/10.1016/j.enggeo.2008.03.014

Filipponi F (2019) Exploitation of Sentinel-2 Time Series to Map Burned Areas at the National Level: A Case Study on the 2017 Italy Wildfires. Remote Sensing 11:622. https://doi.org/10.3390/rs11060622

Finicelli GF, Confuorto P, Carratù MT, Martire DD (2016) Multivariate Statistical approach vs. Deterministic physically based model for landslide susceptibility assessment. ROL 41/2016: https://doi.org/10.3301/ROL.2016.116

Franceschetti G, Migliaccio M, Riccio D, Schirinzi G (1992) SARAS - A synthetic aperture radar (SAR) raw signal simulator. IEEE Transactions on Geoscience and Remote Sensing 30:110–123. https://doi.org/10.1109/36.124221

Freitas C da C, Soler L de S, Sant'Anna SJS, et al (2008) Land Use and Land Cover Mapping in the Brazilian Amazon Using Polarimetric Airborne P-Band SAR Data. IEEE Transactions on Geoscience and Remote Sensing 46:2956–2970. https://doi.org/10.1109/TGRS.2008.2000630

Frost VS, Stiles JA, Shanmugan KS, Holtzman JC (1982) A Model for Radar Images and Its Application to Adaptive Digital Filtering of Multiplicative Noise. IEEE Transactions on Pattern Analysis and Machine Intelligence PAMI-4:157–166. https://doi.org/10.1109/TPAMI.1982.4767223

Fukunaga K, Hostetler L (1975) The estimation of the gradient of a density function, with applications in pattern recognition. IEEE Transactions on Information Theory 21:32–40. https://doi.org/10.1109/TIT.1975.1055330

Fusco, F., De Vita, P., Mirus, B. B., Baum, R. L., Allocca, V., Tufano, R., ... & Calcaterra, D. (2019). Physically based estimation of rainfall thresholds triggering shallow landslides in volcanic slopes of Southern Italy. Water, 11(9), 1915

Gabriel AK, Goldstein RM, Zebker HA (1989) Mapping small elevation changes over large areas: Differential radar interferometry. Journal of Geophysical Research: Solid Earth 94:9183–9191. https://doi.org/10.1029/JB094iB07p09183

Gariano SL, Guzzetti F (2016) Landslides in a changing climate. Earth-Science Reviews 162:227–252. https://doi.org/10.1016/j.earscirev.2016.08.011

Guerriero L, Confuorto P, Calcaterra D, et al (2019) PS-driven inventory of town-damaging landslides in the Benevento, Avellino and Salerno Provinces, southern Italy. Journal of Maps 15:619–625. https://doi.org/10.1080/17445647.2019.1651770

Guzzetti F, Mondini AC, Cardinali M, et al (2012) Landslide inventory maps: New tools for an old problem. Earth-Science Reviews 112:42–66. https://doi.org/10.1016/j.earscirev.2012.02.001

Hungr O, Leroucil S, Picarelli L (2014) The Varnes classification of landslide types, an update. Landslides 11:167–194

ISPRA (2018) Landslides and floods in Italy: hazard and risk indicators. Summary report 2018. Accessed 9 February 2022.

Kyriou, A., & Nikolakopoulos, K. (2018). Assessing the suitability of Sentinel-1 data for landslide mapping. European Journal of Remote Sensing, 51(1), 402-411

Kropatsch WG, Strobl D (1990) The generation of SAR layover and shadow maps from digital elevation models. IEEE Transactions on Geoscience and Remote Sensing 28:98–107. https://doi.org/10.1109/36.45752

Lombardo L, Cama M, Conoscenti C, et al (2015) Binary logistic regression versus stochastic gradient boosted decision trees in assessing landslide susceptibility for multiple-occurring landslide events: application to the 2009 storm event in Messina (Sicily, southern Italy). Nat Hazards 79:1621–1648. https://doi.org/10.1007/s11069-015-1915-3

Miele P, Di Napoli M, Guerriero L, et al (2021) Landslide Awareness System (LAwS) to Increase the Resilience and Safety of Transport Infrastructure: The Case Study of Pan-American Highway (Cuenca–Ecuador). Remote Sensing 13:1564. https://doi.org/10.3390/rs13081564

Momsen E, Metz M (2017) i.segment

Mondini AC (2017) Measures of Spatial Autocorrelation Changes in Multitemporal SAR Images for Event Landslides Detection. Remote Sensing 9:554. https://doi.org/10.3390/rs9060554

Mondini AC, Chang K-T, Chiang S-H, et al (2017) Automatic mapping of event landslides at basin scale in Taiwan using a Montecarlo approach and synthetic land cover fingerprints. International Journal of Applied Earth Observation and Geoinformation 63:112–121. https://doi.org/10.1016/j.jag.2017.07.016

Mondini AC, Santangelo M, Rocchetti M, et al (2019) Sentinel-1 SAR Amplitude Imagery for Rapid Landslide Detection. Remote Sensing 11:760. https://doi.org/10.3390/rs11070760

Morra V, Calcaterra D, Cappelletti P, et al (2010) Urban geology: relationships between geological setting and architectural heritage of the Neapolitan area. Journal of the Virtual Explorer 36:. https://doi.org/10.3809/jvirtex.2010.00261

Notti D, Herrera G, Bianchini S, et al (2014) A methodology for improving landslide PSI data analysis. International Journal of Remote Sensing 35:2186–2214. https://doi.org/10.1080/01431161.2014.889864

Notti D, Meisina C, Zucca F, Colombo A (2012) Models To Predict Persistent Scatterers Data Distribution And Their Capacity To Register Movement Along The Slope. 697:90

Novellino A, Cesarano M, Cappelletti P, et al (2021) Slow-moving landslide risk assessment combining Machine Learning and InSAR techniques. CATENA 203:105317. https://doi.org/10.1016/j.catena.2021.105317

Novellino A, Cigna F, Sowter A, et al (2017) Exploitation of the Intermittent SBAS (ISBAS) algorithm with COSMO-SkyMed data for landslide inventory mapping in north-western Sicily, Italy. Geomorphology 280:153–166. https://doi.org/10.1016/j.geomorph.2016.12.009

Novellino A, De Agostini A, Di Martire D, et al (2015) Using Data from Multiple SAR Sensors in Landslide Characterization: Case Studies from Different Geomorphological Contexts in Italy. In: Lollino G, Giordan D, Crosta GB, et al. (eds) Engineering Geology for Society and Territory - Volume 2. Springer International Publishing, Cham, pp 395–398

Novellino A, Mansour M, Wang L (2020) Measuring soil moisture with spaceborne synthetic aperture radar data. http://nora.nerc.ac.uk/id/eprint/528355/. Accessed 5 Oct 2021

Oliver C, Quegan S (2004) Understanding Synthetic Aperture Radar Images. SciTech Publishing

Plank S, Singer J, Minet C, Thuro K (2012) Pre-survey suitability evaluation of the differential synthetic aperture radar interferometry method for landslide monitoring. International Journal of Remote Sensing 33:6623–6637. https://doi.org/10.1080/01431161.2012.693646

Plank S, Twele A, Martinis S (2016) Landslide Mapping in Vegetated Areas Using Change Detection Based on Optical and Polarimetric SAR Data. Remote Sensing 8:307. https://doi.org/10.3390/rs8040307

Qi Z, Yeh AG-O, Li X, Lin Z (2012) A novel algorithm for land use and land cover classification using RADARSAT-2 polarimetric SAR data. Remote Sensing of Environment 118:21–39. https://doi.org/10.1016/j.rse.2011.11.001

Raspini F, Bardi F, Bianchini S, et al (2017) The contribution of satellite SAR-derived displacement measurements in landslide risk management practices. Nat Hazards 86:327–351. https://doi.org/10.1007/s11069-016-2691-4

Reichenbach P, Rossi M, Malamud BD, et al (2018) A review of statistically-based landslide susceptibility models. Earth-Science Reviews 180:60–91. https://doi.org/10.1016/j.earscirev.2018.03.001

Rolandi G, De Natale G, Kilburn RJC, Troise C, Somma R, Di Lascio M, Fedele A, Rolandi R (2020) The 39 ka Campanian Ignimbrite eruption: new data on source area in the Campanian Plain. Vesuvius, Campi Flegrei, and Campanian Volcanism. https://doi.org/10.1016/B978-0-12-816454-9.00008-0

Saroli M, Stramondo S, Moro M, Doumaz F (2005) Movements detection of deep seated gravitational slope deformations by means of InSAR data and photogeological interpretation: northern Sicily case study. Terra Nova 17:35–43. https://doi.org/10.1111/j.1365-3121.2004.00581.x

Scarpati C, Perrotta A, Lepore S, Calvert A (2013) Eruptive history of Neapolitan volcanoes: constraints from 40Ar–39Ar dating. Geological Magazine 150:412–425. https://doi.org/10.1017/S0016756812000854

Scarpati C, Perrotta A, Sparice D (2015) Volcanism in the city of Naples. ROL 33/2015: https://doi.org/10.3301/ROL.2015.21

Segoni S, Tofani V, Rosi A, et al (2018) Combination of Rainfall Thresholds and Susceptibility Maps for Dynamic Landslide Hazard Assessment at Regional Scale. Front Earth Sci 6:. https://doi.org/10.3389/feart.2018.00085

Shimada M, Watanabe M, Kawano N, et al (2014) Detecting Mountainous Landslides by SAR Polarimetry: A Comparative Study Using Pi-SAR-L2 and X-band SARs. Transactions of the Japan Society for Aeronautical and Space Sciences, Aerospace Technology Japan 12:Pn_9-Pn_15. https://doi.org/10.2322/tastj.12.Pn_9

Solari L, Del Soldato M, Raspini F, et al (2020) Review of Satellite Interferometry for Landslide Detection in Italy. Remote Sensing 12:1351. https://doi.org/10.3390/rs12081351

Spinetti C, Bisson M, Tolomei C, et al (2019) Landslide susceptibility mapping by remote sensing and geomorphological data: case studies on the Sorrentina Peninsula (Southern Italy). GIScience & Remote Sensing 56:940–965. https://doi.org/10.1080/15481603.2019.1587891

Stumpf A, Malet J-P, Delacourt C (2017) Correlation of satellite image time-series for the detection and monitoring of slow-moving landslides. Remote Sensing of Environment 189:40–55. https://doi.org/10.1016/j.rse.2016.11.007

Tang J (2010) A color image segmentation algorithm based on region growing. In: 2010 2nd International Conference on Computer Engineering and Technology. pp V6-634-V6-637

Tao W, Jin H, Zhang Y (2007) Color Image Segmentation Based on Mean Shift and Normalized Cuts. IEEE Transactions on Systems, Man, and Cybernetics, Part B (Cybernetics) 37:1382–1389. https://doi.org/10.1109/TSMCB.2007.902249

Tarquini S, Isola I, Favalli M, et al (2007) TINITALY/01: a new Triangular Irregular Network of Italy

van Westen CJ, van Asch TWJ, Soeters R (2006) Landslide hazard and risk zonation—why is it still so difficult? Bull Eng Geol Environ 65:167–184. https://doi.org/10.1007/s10064-005-0023-0

Wasowski J, Bovenga F (2014) Investigating landslides and unstable slopes with satellite Multi Temporal Interferometry: Current issues and future perspectives. Engineering Geology 174:103–138. https://doi.org/10.1016/j.enggeo.2014.03.003

Wilkinson PL, Anderson MG, Lloyd DM (2002) An integrated hydrological model for rain-induced landslide prediction. Earth Surface Processes and Landforms 27:1285–1297. https://doi.org/10.1002/esp.409

Yin G, Luo J, Niu F, et al (2021) Machine learning-based thermokarst landslide susceptibility modeling across the permafrost region on the Qinghai-Tibet Plateau. Landslides 18:2639–2649. https://doi.org/10.1007/s10346-021-01669-7

Zhang Y, Wu W, Qin Y, et al (2020) Mapping Landslide Hazard Risk Using Random Forest Algorithm in Guixi, Jiangxi, China. ISPRS International Journal of Geo-Information 9:695. https://doi.org/10.3390/ijgi9110695